Harmonizing Nature: Balancing Predators, Prey, and Sustainability in Coldwater Ecosystems

David Perez-Cruet, Langa Siziba, and Mia Wright

Harvard College

***Abstract*—As global weather patterns increase in intensity alongside an increasing demand for seafood, proper management is essential in maintaining healthy fisheries and aquatic ecosystems. Properly assessing, interpreting, and maintaining population dynamics is vital for managing ecosystem dynamics. Specifically, this report analyzes the population dynamics of a large freshwater ecosystem composed of native salmon and whitefish as well as invasive lake trout. The lake trout and salmon compete to prey on the whitefish, and recreational and commercial fishermen harvest all three species. The mathematical model has its foundation in the Lotka-Volterra predator-prey model, while the control mechanism is the harvest of each species. The objective is to maintain robust, healthy populations of salmon and whitefish while minimizing the impact of lake trout. Through the use of MATLAB's Control Design Toolbox, the model indicated that managing the fishing and harvest of a system could lead to stable ecosystem dynamics.**

I. Introduction

Among an increasing intensity of environmental factors contributing to aquatic ecosystem degradation, consumption demands for seafood are growing [5]. To project population dynamics of aquatic species and prevent the overharvesting of these resources, proper models and analysis are essential. Regulations are required to ensure sustainable management practices through correct interpretation of such models. [1]. Aquaculture, commercial fishing, and recreational fishing all impact fish populations, in addition to adverse environmental impacts such as coral bleaching, hydroelectric dam construction, and pollution [5].

Biologists are responsible for developing dynamic models for analyzing aquatic ecosystems on local to global scales [7]. Population dynamics in fish species are heavily dependent on ecosystems and fish life cycles. A coho salmon that starts life in an inland Alaska stream travels to the ocean to mature, then returns to the same stream to spawn three years later encounters different environmental factors than an aquaculture-raised tilapia [1]. Likewise, a coastal migration zone provides different ecosystem dynamics than a geographically isolated alpine lake. Fisheries biologists must determine how to weigh the parsimony versus fidelity of their dynamical system. Parsimony involves simplifying models to make them easier to understand and more adaptable to changing environmental conditions by consolidating system impacts. It seeks to minimize error by reducing complexity. Fidelity intends to replicate the actual conditions with as few approximations as possible to model the real world. An ecosystem dynamics system with high fidelity may consider more factors like weather, inter-species dynamics, and human influence.

With this context in mind, our project expands upon this dynamic modeling endeavor to dissect the intricate interplay within a coldwater ecosystem, home to salmon, whitefish, and an invasive species, lake trout. This ecosystem is riddled with predator-prey interactions, where both salmon and lake trout prey upon the whitefish—a cornerstone species crucial for the ecosystem's balance and human consumption [6]. At the helm of ecosystem management stands the external control input: fish harvesting quotas, pivotal in steering sustainable fishing practices.

In this paper, we systematically explore control aspects in a coldwater ecosystem's dynamics. We start by analyzing the control problem, gradually moving from a broad overview to specific details while balancing simplicity and accuracy. Using an ODE model in Matlab, we examine the system's dynamics, equilibrium points, and behavior under different conditions. Linearization is employed to understand system performance and limitations.

The paper then focuses on designing a feedback control mechanism, considering various controllers' impact on disturbance rejection and measurement noise. It analyzes closed-loop system characteristics, including transfer functions and stability under different control gains. Furthermore, it delves into PID control design, extensively evaluating system performance, stability, and response under varying parameters. It also details the design of a tailored feedback control mechanism to meet specific performance criteria.

The overarching objective of our modeling endeavor is to achieve stability within this complex ecosystem. We aim to foster sustainable populations of salmon and whitefish while mitigating the detrimental effects of lake trout predation. Achieving this equilibrium not only facilitates responsible recreational fishing but also seeks to alleviate harvesting strains on these populations.

II. System Modeling

Our model will consider natural predator-prey interactions between the salmon and whitefish and the impact of an invasive species: lake trout. The salmon and lake trout both prey on the whitefish. The external control input on the system will be fish harvesting quotas to help manage sustainable fishing practices. The output will be the populations of all three species. Ideally, our coldwater ecosystem will reach stable populations of salmon and whitefish while minimizing

Parameter	Value
g_w	Growth rate of the whitefish
g_s	Growth rate of the salmon
g_l	Growth rate of the lake trout
d_w	Natural death rate of the whitefish
d_s	Natural death rate of the salmon
d_l	Natural death rate of the lake trout
f_s	Feeding constant of the salmon
f_l	Feeding constant of the lake trout
K_w	Carrying capacity of the whitefish

TABLE I: Parameters used in system model

the negative impact of lakefish predation. It will facilitate responsible recreational fishing and will be able to stabilize harvesting strains on the population. To ensure fidelity, we will include the specific factors that modulate fish harvesting intensity, which we can eventually adapt to model seasonal patterns, including weather and fish spawning. We will have three states: the populations of all three species. To ensure parsimony, we will structure our dynamical system around widely-accepted predator-prey system models [2], and consider the system isolated with only three species.

A. System Model

We developed a model to predict the future population dynamics of each species using the past and present output of the populations. The model developed aims to predict the population dynamics of species in a coldwater ecosystem by considering their interactions and control measures.

The system's control mechanisms regulate each species' population. Salmon and lake trout populations grow proportionally to their interactions with whitefish, modulated by growth coefficients g_s and g_l respectively. Both predators face death rates (d_s for salmon and d_l for lake trout) reducing their population growth. Whitefish population change is boosted by a growth rate g_w towards a carrying capacity K_w, while their population decreases due to interactions with the predator species.

The system model is described through differential equations, defining the rates of change for whitefish ($W(t)$), salmon ($S(t)$), and lake trout ($L(t)$) populations. These equations involve growth, death rates, and interactions among the species. The model without external input can be represented as follows:

Our system model is as follows:

- State: Current fish populations $\begin{pmatrix} W(t) : Whitefish \\ S(t) : Salmon \\ L(t) : LakeTrout \end{pmatrix}$
- Output: Fish populations $\begin{pmatrix} W(t) \\ S(t) \\ L(t) \end{pmatrix}$

We can then write our system as a system of differential equations:

$$\begin{aligned} \frac{dW(t)}{dt} &= (g_w - d_w)W(t)\left(1 - \frac{W(t)}{K_w}\right) - f_sS(t) - f_lL(t) \\ \frac{dS(t)}{dt} &= g_sS(t)\left(1 - \frac{S(t)}{W(t)+1}\right) - d_sS(t) \\ \frac{dL(t)}{dt} &= g_lL(t)\left(1 - \frac{L(t)}{W(t)+1}\right) - d_lL(t)t \end{aligned}$$

However, there is an external input of fish harvesting. This rate depends on various factors such as regulations, fishing efforts, environmental conditions, or management policies. It could be constant over time vary seasonally, or respond to the population size itself (e.g., harvesting proportional to population size). Hence in a bid to maintain parsimony by simplifying our system, we sacrifice some degrees of accuracy. The harvest rate can be represented as follows:

$$\text{Harvest of each species } H(t) = \begin{pmatrix} H_w(t) \\ H_s(t) \\ H_l(t) \end{pmatrix}$$

The system becomes:

$$\begin{aligned} \frac{dW(t)}{dt} &= (g_w - d_w)W(t)\left(1 - \frac{W(t)}{K_w}\right) - f_sS(t) - f_lL(t) - H_w(t) \\ \frac{dS(t)}{dt} &= g_sS(t)\left(1 - \frac{S(t)}{W(t)+1}\right) - d_sS(t) - H_s(t) \\ \frac{dL(t)}{dt} &= g_lL(t)\left(1 - \frac{L(t)}{W(t)+1}\right) - d_lL(t) - H_l(t) \end{aligned}$$

The control input (u) signifies the interventions or adjustments biologists can make, specifically monitoring and managing the fish populations' harvest.

B. Standard State-Space Form

The system can be represented in standard state-space form, collapsing the states into a vector x and expressing the differential equations in terms of x_1, x_2, and x_3, corresponding to whitefish, salmon, and lake trout populations respectively. The state-space model reflects the system's dynamics and control input (u), which denotes the harvest of each species. The three states represent the populations of the species, while the output mirrors the input as a means to monitor and adjust harvest regulations for desired populations.

Our system model is as follows:

- Control Input u(t) : Harvest of each species

  $$u = \begin{pmatrix} \frac{H_w(t)}{\alpha} \\ \frac{H_s(t)}{\beta} \\ \frac{H_l(t)}{\gamma} \end{pmatrix}$$

  Where α, β, γ are functions that relate the input to the Harvesting. These rely on season, weather, fish spawning activity, harvest intensity, consumer demand, and so on.

However, for simplicity, we set them to $\alpha = \beta = \gamma = 1$.

- State x(t) : Current fish populations

$$x = \begin{pmatrix} W(t) \\ S(t) \\ L(t) \end{pmatrix}$$

- Output y(t) : Fish populations

$$y = \begin{pmatrix} W(t) \\ S(t) \\ L(t) \end{pmatrix}$$

We can express the system's evolution by incorporating the harvesting rates $H(t)$ into the differential equations using the control input $u(t)$. We can then write our system as a system of differential equations. Collapsing the states into the vector x, we have:

$$\begin{bmatrix} \dot{W}(t) \\ \dot{S}(t) \\ \dot{L}(t) \end{bmatrix} = \begin{bmatrix} (g_w - d_w)W(t)\left(1 - \frac{W(t)}{K_w}\right) - f_s S(t) - f_l L(t) - u_w(t) \\ g_s S(t)\left(1 - \frac{S(t)}{W(t+1)}\right) - d_s S(t) - u_s(t) \\ g_l L(t)\left(1 - \frac{L(t)}{W(t)+1}\right) - d_l L(t) - u_l(t) \end{bmatrix}$$

The model can then be written in standard form as:

$$\begin{cases} \dot{x} = \begin{bmatrix} (g_w - d_w)x_1(1 - \frac{x_1}{K_w}) - f_s x_2 - f_l x_3 - u_w \\ g_s x_2(1 - \frac{x_2}{x_1+1}) - d_s x_2 - u_s \\ g_l x_3(1 - \frac{x_3}{x_1+1}) - d_l x_3 - u_l \end{bmatrix}, \\ y = \begin{bmatrix} x_1 \\ x_2 \\ x_3 \end{bmatrix} \end{cases}$$

The above represents our state-space model wherein the control input reflects the interventions biologists can implement within the system—specifically, the monitoring and management of fish population harvests. This model encapsulates three primary states: the salmon population, the whitefish population, and the lake trout population. Remarkably, the output mirrors the input, underlining the expectation that biologists can observe population variations pre- and post-harvest, and then adapt harvest regulations to achieve desired population levels.

It's essential to note the model's simplification, which considers only three interacting species while overlooking external factors such as weather impacts, potential shifts in death rates corresponding to different life cycle stages, or the influence of recreational fishing practices on population dynamics. Moreover, this model assumes direct predation as the sole factor influencing population growth or decline. Furthermore, constant death rates are assumed. Notably, the harvest rates do not account for the impact of recreational catch-and-release fishing, which, while intended to return fish safely to the ecosystem unharmed, may affect the population dynamics.

Parameter	Value
g_w	1.5 (whitefish per day) [4]
g_s	1.25 (salmon per day) [4]
g_l	1.29 (lake trout per day) [12]
d_w	0.6 (whitefish per day) [6]
d_s	0.83 (salmon per day) [4]
d_l	0.6 (lake trout per day) [12]
K_w	$7,740,000$ (whitefish) [6]
f_s	0.5 (success rate) [6]
f_l	0.7 (success rate) [6]

TABLE II: List of plausible parameter values for the given system

C. *Plausible parameter values*

In developing our model, we selected parameters by drawing from scientific papers and available research. These parameters served as the backbone of our model, allowing us to simulate behaviors closely resembling those observed in natural systems. By anchoring our model in empirical data and established scientific knowledge, we aimed to create a robust foundation mirroring real-world phenomena. This approach not only bolstered the accuracy of our model but also empowered us to predict and test scenarios effectively. Furthermore, validation against empirical observations reinforced the reliability of our model, providing deeper insights into the complexities of the systems we studied.

D. *Simulation and Analysis of Dynamic Behavior ($u = 0$)*

To comprehend the nuanced behavior within our model, we aim to simulate specific points of interest. This targeted approach allows us to explore scenarios that highlight critical dynamics in the system, including extreme cases like the absence of a particular fish species. The following starting points represent instances of particular interest within our model:

1) Staring point 1: The dynamic behavior of all fish present at a random state

$$x_{o1} = \begin{pmatrix} 1000000 \\ 500000 \\ 300000 \end{pmatrix}$$

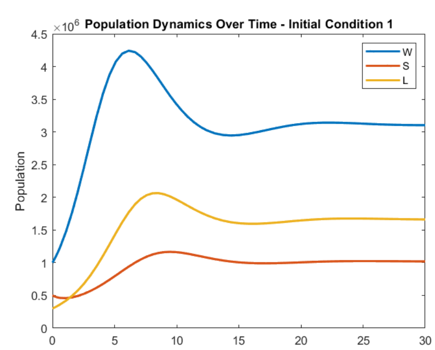

““““

Fig. 1: Using x_{o1} as initial value

2) Starting point 2: The dynamic behavior in the absence of whitefish

$$x_{o2} = \begin{pmatrix} 0 \\ 500000 \\ 300000 \end{pmatrix}$$

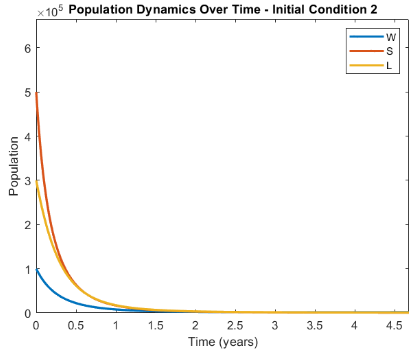

Fig. 2: Simulating dynamic behavior with x_{o2} as initial value

3) Starting point 3: The dynamic behavior of whitefish and trout in the absence of the salmon

$$x_{o3} = \begin{pmatrix} 1000000 \\ 0 \\ 300000 \end{pmatrix}$$

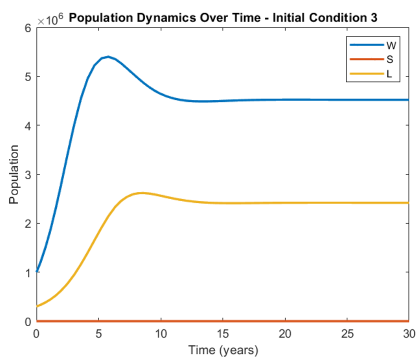

Fig. 3: Simulating dynamic behavior with x_{o3} as initial value

4) Starting point 4: The dynamic behavior of whitefish and salmon in the absence of the salmon

$$x_{o4} = \begin{pmatrix} 1000000 \\ 500000 \\ 0 \end{pmatrix}$$

5) Starting point 5: The dynamic behavior of all fish at zero

$$x_{o5} = \begin{pmatrix} 0 \\ 0 \\ 0 \end{pmatrix}$$

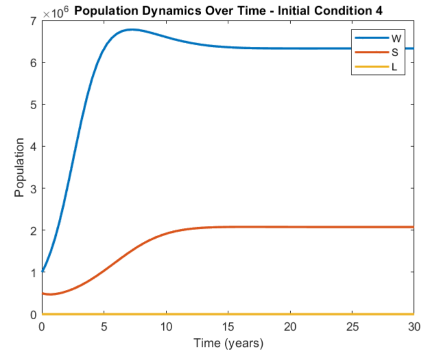

Fig. 4: Simulating dynamic behavior with x_{o4} as initial value

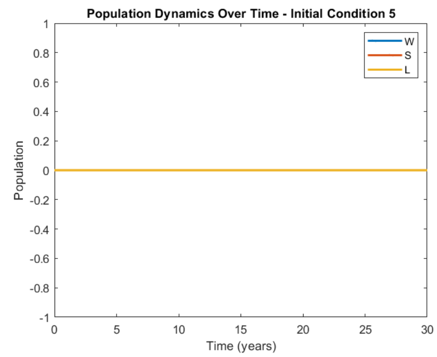

Fig. 5: Simulating dynamic behavior with x_{o5} as initial value

6) Starting point 6: The dynamic behavior of whitefish in the absence of predators.

$$x_{o6} = \begin{pmatrix} 1000000 \\ 0 \\ 0 \end{pmatrix}$$

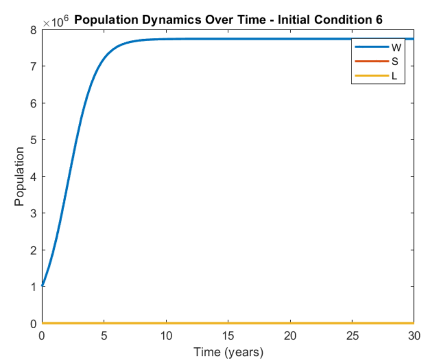

Fig. 6: Simulating dynamic behavior with x_{o6} as initial value

In scenarios where predators were absent from the system, the Whitefish population exhibited robust growth, following a logistic curve until it reached a carrying capacity dictated by K_w. This aligns with expectations, indicating that in the absence of predation, prey populations can grow exponentially until environmental limits are reached.

Conversely, when the whitefish population was initialized at zero while the predator populations maintained non-zero values, the model predicted an exponential decline in the predator populations. Devoid of a prey base, the predators' populations declined steadily over time.

Furthermore, initializing any population at zero resulted in that population remaining at zero throughout the simulation. Interestingly, when whitefish was absent while the predator populations exponentially decreased to zero, the model displayed signs of instability. This instability suggests a disruption in the ecological balance, potentially leading to erratic behaviors in the predator populations.

Additionally, when one predator population was initialized at zero while the other predator and prey populations started non-zero, the model exhibited typical predator-prey dynamics between the remaining predator and prey populations. This behavior resembled the expected interactions seen in simpler one-predator one-prey systems.

The simulations unveiled distinctive population dynamics contingent upon different initial conditions. The absence or presence of specific populations had discernible impacts on the model's trajectories, showcasing the intricate interdependencies inherent in predator-prey ecosystems.

Further investigations could delve deeper into understanding the thresholds or conditions leading to instability in the model. Exploring these factors may provide deeper insights into the stability and resilience of predator-prey relationships within ecosystems.

E. Impact of Parameter Changes on Predator-Prey Dynamics

The predator-prey model examines the interactions between Whitefish (prey), Salmon, and Lake Trout (predators). This report explores how altering specific parameters within the model influences the behaviors of these populations.

Parameter Modifications and Expected Behaviors:

Growth Rate of Prey (Whitefish): Changing the growth rate (g_w) of Whitefish will directly impact its population dynamics. An increase in g_w would likely result in a more rapid rise in the Whitefish population, potentially causing accelerated fluctuations in predator populations. Conversely, decreasing g_w would slow down Whitefish population growth, potentially leading to delayed or subdued oscillations among predators.

Growth Rates of Predators (Salmon and Lake Trout): Modifying the growth rates (g_s and g_l) of predators can significantly influence predator-prey dynamics. Higher g_s or g_l could intensify predator behavior, causing quicker depletion of Whitefish populations and more erratic oscillations among all populations. Conversely, reducing g_s or g_l might slow the decline of Whitefish populations, resulting in smoother and more stable predator-prey dynamics.

Death Rates of Predators: The death rates (d_s and d_l) of predators play a crucial role in population control. Elevated death rates could decrease predator populations, leading to a slower decline in Whitefish populations and increased stability. Conversely, lower death rates might intensify the impact on Whitefish populations, potentially causing more pronounced fluctuation.

Carrying Capacity of Whitefish (K_w): Adjusting the carrying capacity (K_w) influences the maximum Whitefish population size before leveling off. Increasing K_w might sustain higher Whitefish populations, leading to more stable predator populations. Conversely, reducing K_w could result in quicker stabilization at lower levels, potentially causing earlier collapses or more frequent oscillations in predator populations.

Alterations in specific parameters within the predator-prey model distinctly influence population behaviors. Understanding the impacts of these parameter changes provides insights into the delicate balance and dynamics of predator-prey ecosystems.

F. Simulation and Analysis of Dynamic Behavior with input(u)

This section investigates the impact of harvesting rates on the population dynamics within this ecosystem.

The dynamic behavior of all fish present at a random state

$$x_{o1} = \begin{pmatrix} 1000000 \\ 500000 \\ 300000 \end{pmatrix}$$

$$u = \begin{pmatrix} 100000 \\ 50000 \\ 30000 \end{pmatrix}$$

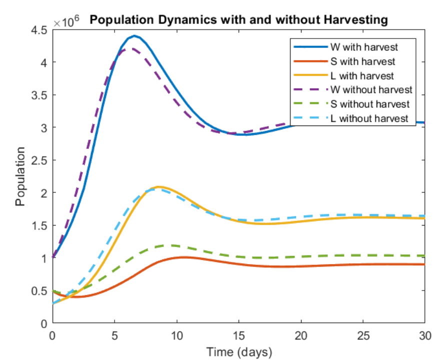

‘‘‘‘‘

Fig. 7: Using x_{o1} as initial value

Simulation Results: The simulation was conducted for a period of 30 years, considering two scenarios:

With Harvesting:
The model was simulated with harvesting rates for Whitefish, Salmon, and Lake Trout (W, S, L) at rates of 100,000, 50,000, and 30,000, respectively. The population dynamics depicted distinct behaviors, showing stability point affected by the harvesting pressure on each species. Whitefish populations experienced a more pronounced decline, impacting the predator populations.

Without Harvesting:
In the absence of harvesting (setting the rates to zero), the population dynamics showed stable behaviors.
The graph illustrates the population dynamics of W, S, and L with and without harvesting on the same axis. The presence of

harvesting resulted in a smaller stable population, particularly noticeable in salmon populations.

III. Linearization and Stability

A. Equilibrium Points

To determine the equilibrium point(s) under the assumption of zero input ($u = 0$), the first step involves setting all-time derivatives to zero to find the equilibrium values W^*, S^*, and L^*. This process entails solving the system of equations resulting from setting the derivatives to zero, as follows:

$$0 = g_w x_1^* \left(1 - \frac{x_1^*}{K_w}\right) - f_s x_2^* - f_l x_3^*$$
$$0 = g_s x_2^* \left(1 - \frac{x_2^*}{x_1^* + 1}\right) - d_s x_2^*$$
$$0 = g_l x_3^* \left(1 - \frac{x_3^*}{x_1^* + 1}\right) - d_l x_3^*$$

Solving this system of equations yields the equilibrium points (x_1^*, x_2^*, x_3^*), and in this case, six such equilibrium points are obtained. These points represent stable or steady-state values where the rates of change of the variables are zero, given no external inputs ($u = 0$). Determining these equilibrium points provides valuable insights into the behavior of the system in the absence of external influences or inputs.

The calculated equilibrium points are as follows:

$$\begin{bmatrix} 0 & 0 & 0 \\ 7740000 & 0 & 0 \\ 0 & 0 & 0 \\ 6295199 & 2115187 & 0 \\ 1 & 0 & 1 \\ 4520000 & 0 & 2417675 \\ 2 & 1 & 1 \\ 3075198 & 1033267 & 1644874 \end{bmatrix}$$

Our model aims to focus on the stability of all three fish species, while minimizing the impact of lake trout. Therefore, the fourth equilibrium point represents the ideal ecosystem dynamics in the absence of any historical human intervention. However, in the absence of the control input, harvest, nonzero populations of all three species are expected to be nonzero. In other words, it is assumed that lake trout have already been introduced, whether naively, unintentionally, or otherwise. Resultingly, the lake trout have established a viable, if not dominant, population. This necessitates the exclusion of trivial solutions where any individual fish species reaches zero or its carrying capacity while others diminish. Thus, a singular equilibrium point of particular interest is one where all three fish species coexist with non-zero, non-maximal populations:

$$x^* \approx \begin{pmatrix} 3075198 \\ 1033267 \\ 1644874 \end{pmatrix}$$

This equilibrium point corresponds to:

$$y^* \approx \begin{pmatrix} 3075198 \\ 1033267 \\ 1644874 \end{pmatrix}$$

This equilibrium point signifies a state where whitefish, salmon, and lake trout populations stably coexist without reaching their maximum capacities or extinction. It represents a balanced ecosystem with sustainable populations of all three fish species.

B. Linearization Around Equilibrium

Linearization is a vital method used to study system behavior around equilibrium points, offering insights into local stability. In our analysis of the predator-prey ecosystem, linearization is performed around the previously identified equilibrium point $x^* \approx \big(3075198, \quad 1033267, \quad 1644874\big)$.

This process involves defining perturbations from the equilibrium: $(x - x^*) = \tilde{x}$ and $(u - u^*) = \tilde{u}$, enabling us to reformulate the differential equations accordingly. The linearized system can be represented as:

$$\dot{\tilde{x}} = A\tilde{x} + B\tilde{u}$$
$$\tilde{y} = C\tilde{x}$$

Linearization aids in analyzing local stability and behavior around an equilibrium point. The Jacobian matrix $J(x)$ at the equilibrium point, often denoted as A in the linearized state, encapsulates the system's behavior near stability.

The general Jacobian matrix is given by:

$$\begin{bmatrix} \frac{9}{10} - \frac{x_1}{4300000} & -\frac{1}{2} & -\frac{7}{10} \\ \frac{5x_2^2}{4(x_1+1)^2} & \frac{21}{50} - \frac{5x_2}{2(x_1+1)} & 0 \\ \frac{129x_3^2}{100(x_1+1)^2} & 0 & \frac{69}{100} - \frac{129x_3}{50(x_1+1)} \end{bmatrix}$$

This matrix sheds light on the linearized behavior at the equilibrium point at the equilibrium point x^*, which dictates the local dynamics:

$$\begin{bmatrix} 0.1848 & -0.5000 & -0.7000 \\ 0.1411 & -0.4200 & 0 \\ 0.3691 & 0 & -0.6900 \end{bmatrix}$$

Additionally, within this linearized predator-prey ecosystem model, the input matrix B and output matrix C are defined as follows:

The input matrix B represents external influences on the rates of change in state variables. In our ecosystem model, B can be expressed as:

$$B = \begin{bmatrix} -1 & 0 & 0 \\ 0 & -1 & 0 \\ 0 & 0 & -1 \end{bmatrix}$$

This signifies that external inputs predominantly impact the dynamics of the lake trout population (x_3) from its equilibrium value.

The output matrix C establishes relationships between state variables and observable outputs in the ecosystem:

$$C = \begin{bmatrix} 1 & 0 & 0 \\ 0 & 1 & 0 \\ 0 & 0 & 1 \end{bmatrix}$$

This matrix indicates direct relationships between observable outputs and population sizes of whitefish (x_1), salmon (x_2), and lake trout (x_3). Linearization enables us to examine disturbances' impacts on the predator-prey ecosystem's stability near equilibrium, providing valuable insights into its dynamic behavior.

C. Evaluating the Stability of the Linearized System

The eigenvalues of the Jacobian matrix are:

$$\lambda \approx \begin{pmatrix} -0.2062 + 0.3995i \\ -0.2062 - 0.3995i \\ -0.5128 \end{pmatrix}$$

Analyzing these eigenvalues allows us to assess the stability of the system's equilibrium point. All real values of the eigenvalues are negative therefore when no input is applied, the system's equilibrium point is determined to be stable.

This analysis suggests that perturbations around this equilibrium point may not lead to instability in the system.

IV. Simulation/Dynamic Behavior around x^*

To assess the dynamic behavior around our equilibrium point of interest, we conducted an ODE simulation with initial conditions slightly above and below the equilibrium point.

1) $x_{o1} = \begin{pmatrix} 295198 \\ 933268 \\ 1544875 \end{pmatrix}$

2) $x_{o2} = \begin{pmatrix} 3175197 \\ 1133266 \\ 1744873 \end{pmatrix}$

Initiating the system with initial conditions both above and below the equilibrium point results in anticipated stability, as depicted in the following graph:

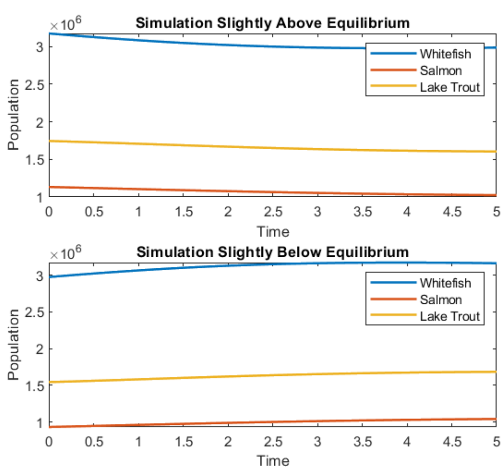

Fig. 8: Simulation with both initial conditions x_{o1} and x_{o2}

The graph illustrates the stable responses from both sets of initial conditions, showing inimization of deviations from the equilibrium point over time.

V. State Feedback Control

A. Control Objective

The objective of this project is to provide mathematical models that help fishery biologists manage ecosystems. To that end, our control objective is to drive our three state model to desired population sizes of the three species. To do so, fishing harvests will be moderated. This will allow recreational and commercial fishermen to harvest fish while maintaining sustainable ecological standards.

Our control objective is to set regulations, or limits, on the harvest of each species. It does not account for the fishability of each species. For example, salmon may be commercially harvested most consistently outside of their autumn spawning season with gill nets in lakes, while recreational harvest prevails in river ecosystems during the spawning season. Similarly, each species presents different challenges for harvest beyond simply population density. For example, whitefish remain in schools, while lake trout are primarily solitary. To simplify our model, our controller will establish the optimal harvest goals to drive out state to the desired population sizes.

Another objective is to achieve effective fish population control while safeguarding the ecological stability of the system. To this end, the chosen eigenvalues and control parameters need to ensure these aspects:

- Preserving System Stability: This element safeguards against instability within the system. Ensuring that the system remains stable under such control inputs is important.
- Controlled Response Without Overshooting: In an ecosystem, overshooting could have adverse ecological consequences. Therefore, our control system must respond with minimal overshoot, reducing the potential ecological impact.
- Gradual Increase for Ecological Harmony: Recognizing the delicate nature of ecosystems, we have prioritized a gradual increase in the system's response. This gradual approach is instrumental in preserving ecological balance. It allows the control system to adapt harmoniously to changes, ensuring that the objectives of fish population control are met without imposing abrupt and disruptive changes to the ecosystem.

B. Reachability

We first need to determine the reachability of the system based on the given parameters and variables. If the system is reachable, it implies the capability to access any point within the state space through specific inputs. Understanding the system's reachability is pivotal for identifying an effective control signal [14].

To establish reachability, we calculate the reachability matrix (W_r), given by:

$$W_r = [B, AB, A^2B]$$

Using the linearized system derived in Section III-A, the reachability matrix can be computed at the equilibrium point of interest:

$$x^* \approx \begin{pmatrix} 3075198 \\ 1033267 \\ 1644874 \end{pmatrix}:$$

$$W_r = \begin{bmatrix} -1 & 0 & 0 & -0.1848 & 0.5 & 0.7 & 0.2947 & -0.1176 & -0.3536 \\ 0 & -1 & 0 & -0.1411 & 0.4200 & 0 & 0.0332 & -0.1058 & 0.0988 \\ 0 & 0 & -1 & -0.3691 & 0 & 0.6900 & 0.1864 & 0.1845 & -0.2178 \end{bmatrix}$$

The computed reachability matrix above exhibits full row rank, indicating $rank(W_r) = 3$. Hence, our system is reachable.

C. Designing Basic Closed-loop Controller

The next step is to design a closed-loop controller for our linearized system. In the context of this system, the control input $u(t)$ can be defined as:

$$u(t) = Kx + kr \cdot r \quad (1)$$

where K represents a vector of controller gains with components $[k_W, k_S, k_T]$, and r denotes the reference value.

With this controller, the state of our system, represented by the vector x, is influenced by both the control input and the reference value. The state variables may encompass various parameters or variables describing the system's behavior. This controller facilitates the regulation and stabilization of the system by adjusting the control input based on the current state and the desired reference value.

The constant gain kr multiplies the reference value r, allowing adjustment of the reference value's impact on the control input. Essentially, it determines the extent to which the controller responds to changes in the reference value. In our case, we would like to control the population of all our fish populations hence kr is a 3×3 matrix

The dynamics of the system can be expressed as:

$$\dot{x} = Ax - B(Kx + kr \cdot r) = (A - BK)x + Bkr \cdot r$$

where A is the system's state matrix, B represents the control input matrix, K is the controller gain matrix, r is the reference value, and kr is the constant gain influencing the reference input.

Making our desired eigenvalues to be:

$$p = [-2, -3 + 1.5i, -3 - 1.5i]$$

we use the MATLAB function $place$ to evaluate the feedback gain matrix.

The feedback gain matrix, denoted as K, is given by:

$$\begin{bmatrix} -3.1768 & -1 & 0.7 \\ 1.3655 & -2.59 & 0 \\ -0.3691 & 0 & -1.31 \end{bmatrix}$$

This matrix is utilized in the closed-loop control system to regulate and stabilize the state variables of the system. It influences the system's response based on the current state and the reference input.

Reference Gain Kr: The reference gain matrix, denoted as kr, is calculated by $K_r = \left(-C \cdot (A - B \cdot K)^{-1} \cdot B\right)^{-1}$. It is represented as:

$$\begin{bmatrix} -3 & -1.5 & 0 \\ 1.5 & -3 & 0 \\ 0 & 0 & -2 \end{bmatrix}$$

This matrix signifies the influence of the reference input on the control system's behavior. It determines how the control input responds to changes in the reference values, assisting in achieving specific performance objectives.

Matrix $\tilde{A} = (A - BK)$:

$$\begin{bmatrix} -3 & -1.5 & 0 \\ 1.5 & -3 & 0 \\ 0 & 0 & -2 \end{bmatrix}$$

This modified state matrix, derived from the original system matrix, reflects the impact of the controller gains on the system's dynamic behavior.

Matrix $\tilde{B} = Bkr$:

$$\begin{bmatrix} 3 & 1.5 & 0 \\ -1.5 & 3 & 0 \\ 0 & 0 & 2 \end{bmatrix}$$

This matrix signifies the relationship between the control input and the reference input after the application of the control gains.

Matrix $\tilde{C}$:

$$\begin{bmatrix} 1 & 0 & 0 \\ 0 & 1 & 0 \\ 0 & 0 & 1 \end{bmatrix}$$

D. Simulation and Analysis of the Dynamics of the Closed-Loop System

To understand the behavior of our closed-loop control system, we conducted an analysis using MATLAB's built-in capabilities, specifically the 'lsim' and 'ss' function. This analysis utilized the 'step' function, a versatile tool designed for exploring and visualizing system dynamics.

In the following code snippet, A denotes the system's state matrix, B represents the control input matrix, K denotes the controller gain matrix, C stands for the output matrix, and D represents the feedforward matrix (which is 0 in our model). The 'step' function played a pivotal role in evaluating our control system's response to a step change in the reference input.

```
sys = ss(A - B * K, B * Kr, C, 0);
[y, t, x] = lsim(sys, u, t);
```

The step response analysis yielded crucial insights into both the transient and steady-state characteristics of our closed-loop system. This assessment enabled us to gauge the system's performance against predefined objectives and facilitated informed adjustments to meet our control goals.

Informed decision-making involves evaluating the step response of the system across various p-values, starting with our pre-selected p-value from the preceding section. Throughout this section, we simulated the step response for four distinct p-values, including the previously chosen one, while adjusting their values to identify a p-value that aligns effectively with our system's behavior.

The p-value structure is as follows:

$$p = [c, a + bi, a - bi]$$

1) $p = [-2, -3 + 1.5i, -3 - 1.5i]$

Feedback Gain Matrix K:

$$\begin{bmatrix} -3.1768 & -1 & 0.7 \\ 1.3655 & -2.59 & 0 \\ -0.3691 & 0 & -1.31 \end{bmatrix}$$

Reference Gain Kr:

$$\begin{bmatrix} -3 & -1.5 & 0 \\ 1.5 & -3 & 0 \\ 0 & 0 & -2 \end{bmatrix}$$

The step response is shown below:

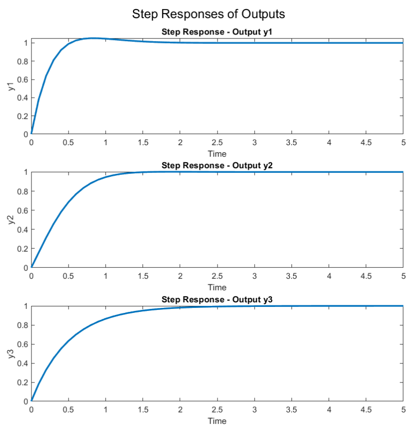

Fig. 9: Step response when $p = p_1$

2) $p = [-2, -10 + 1.5i, -10 - 1.5i]$

Feedback Gain Matrix K:

$$\begin{bmatrix} -10.1768 & -1 & 0.7 \\ 1.3655 & -9.59 & 0 \\ -0.3691 & 0 & -1.31 \end{bmatrix}$$

Reference Gain Kr:

$$\begin{bmatrix} -10 & -1.5 & 0 \\ 1.5 & -10 & 0 \\ 0 & 0 & -2 \end{bmatrix}$$

The step response is shown below:

3) $p = [-1, -3 + 1.5i, -3 - 1.5i]$

Feedback Gain Matrix K:

$$\begin{bmatrix} -3.1768 & -1 & 0.7 \\ 1.3655 & -2.59 & 0 \\ -0.3691 & 0 & -0.31 \end{bmatrix}$$

Reference Gain Kr:

$$\begin{bmatrix} -3 & -1.5 & 0 \\ 1.5 & -3 & 0 \\ 0 & 0 & -1 \end{bmatrix}$$

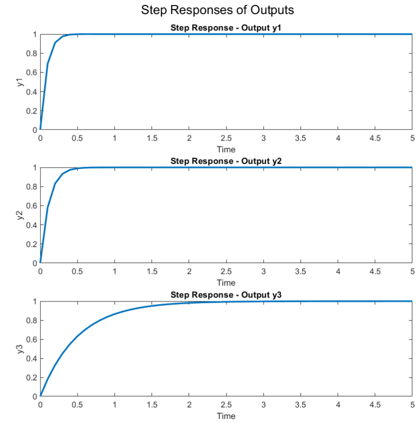

Fig. 10: Step response when $p = p_1$

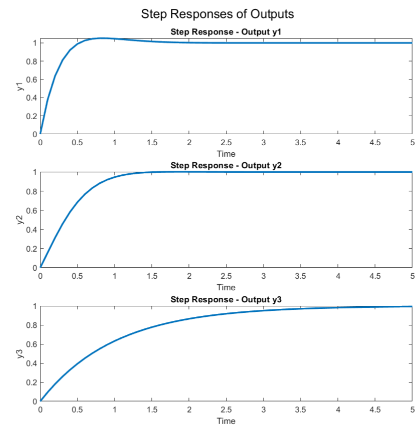

Fig. 11: Step response when $p = p_1$

The step response is shown below:

4) $p = [-2, -3 + 5i, -3 - 5i]$

Feedback Gain Matrix K:

$$\begin{bmatrix} -3.1768 & -4.5 & 0.7 \\ 4.8655 & -2.59 & 0 \\ -0.3691 & 0 & -1.31 \end{bmatrix}$$

Reference Gain Kr:

$$\begin{bmatrix} -3 & -5 & 0 \\ 5 & -3 & 0 \\ 0 & 0 & -2 \end{bmatrix}$$

The step response is shown below:

E. Final Controller based on Closed-Loop System Dynamics

Selecting an appropriate p value for the step response analysis holds significant importance, especially considering the sensitivity of the environment or system under consideration.

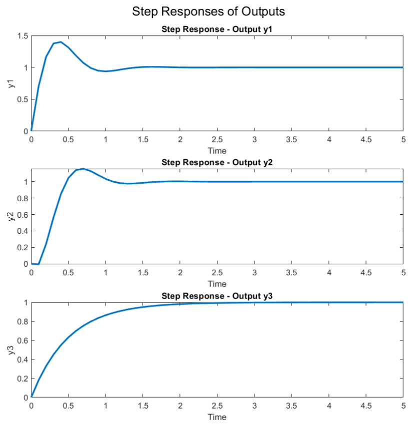

Fig. 12: Step response when $p = p_4$

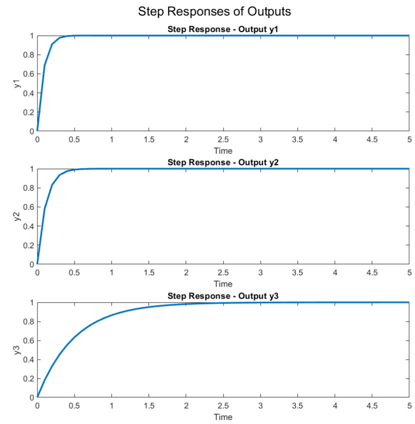

Fig. 13: Step response of our final closed loop

The overshooting observed in the step response graph can have practical implications, particularly in environments sensitive to abrupt changes or fluctuations.

In our analysis, the choice of $p = [-2, -10 + 1.5i, -10 - 1.5i]$ was made after careful consideration of the system's response characteristics. This selection aimed to strike a balance between achieving system stability and minimizing overshooting tendencies. The complex-conjugate nature of the chosen eigenvalues $-10 + 1.5i$ and $-10 - 1.5i$ contributes to a damped response, which aids in curbing overshooting while ensuring a controlled and stable system response.

This specific p value aligns well with our system's behavior and objectives. By evaluating the step response corresponding to this p-value, we observed a response that meets our criteria, demonstrating minimal overshooting while effectively regulating the system towards the desired reference input.

Drawing from our analysis and observations from the previous section, we have successfully established eigenvalues that align with the anticipated general behavior of our control system and our control objectives. These carefully chosen eigenvalues are instrumental in ensuring the stability and performance of the system, striking a delicate balance between control input, which represents fish harvesting, and the system's response.

The step response is shown below:

VI. Output Feedback Control

A. Feedback Control Objectives with Luenberger Observer

Our feedback control objectives, utilizing a Luenberger observer with measurements of all outputs, are important because, with the observer, we can predict hence control the real-life behavior of our system more accurately.

One of the most important objectives is that we would like to maintain state estimation for informed control, regulate species populations to desired levels, and optimize harvest control based on estimated states. Similar to our control objective, it is important to maintain ecosystem stability and ecological impact. Preservation of our system stability and minimization of ecological impact through controlled responses. Hence, we will choose eigenvalues that attain this goal. The observer must have gradual adaptation to changing conditions, ensuring robust control in the face of uncertainties, and achieving convergence for reliable state estimates. Also, we must be able to optimize control inputs to meet population targets and use of adaptive control strategies based on observed dynamics.

These objectives collectively enable us to achieve effective fish population control while safeguarding the ecological stability of the system.

B. Observability

The output of the system is the population of all three fish species. Thus, the C Matrix is:

$$\begin{bmatrix} 1 & 0 & 0 \\ 0 & 1 & 0 \\ 0 & 0 & 1 \end{bmatrix}$$

To certify if the information given in $y(t)$ and $u(t)$ are enough to determine the state $x(t)$ for any value of t, the observability of the system is calculated using the observability matrix W_o, where

$$W_o = [C, CA, CA^2]^T$$

If $rank(W_o) = 3$, then the system is observable for the given input and output.

Inputing the C and A matrices into the above equation yields

$$W_o = \begin{bmatrix} 1 & 0 & 0 \\ 0 & 1 & 0 \\ 0 & 0 & 1 \\ 0.1848 & -0.5000 & -0.7000 \\ 0.1411 & -0.4200 & 0 \\ 0.3691 & 0 & -0.6900 \\ -0.2947 & 0.1176 & 0.3536 \\ -0.0332 & 0.1058 & -0.0988 \\ -0.1864 & -0.1845 & 0.2178 \end{bmatrix}$$

Given $Rank(W_o) = 3$, it indicates the system is observable for the specified input and output.

C. State Estimation

Consider a system described by equations that track how its state and outputs change over time:

$$\frac{dx}{dt} = Ax + Bu, \quad y = Cx$$

This system is observable, meaning its internal state can be deduced from its outputs. To estimate this state ($\hat{x}$), an additional system is created, the observer:

$$\frac{d\hat{x}}{dt} = A\hat{x} + Bu + L(y - C\hat{x})$$

Here, $\hat{x}$ represents the estimated state, and $L = [l_w, l_s, l_t]^T$ is the matrix determining how much importance to assign to the difference between the actual output (y) and the estimated output ($C\hat{x}$).

The difference between the real state (x) and the estimated state ($\hat{x}$) is termed the observer error ($e = x - \hat{x}$). The dynamics of this error are given by:

$$\dot{e} = \dot{x} - \dot{\hat{x}} = (A - LC)e$$

Here, $A_e = (A - LC)$ represents the dynamics of the error.

To calculate the matrix L, MATLAB's `place()` function is employed, allowing the selection of appropriate values to stabilize the system. In this case, the chosen values ($p = [-2, -3 + 1.5i, -3 - 1.5i]$) aim to stabilize the observer. Utilizing the provided system matrices (A, B, and λ), the estimator gain matrix is found to be:

$$L = \begin{pmatrix} 7.0486 \\ -0.0105 \\ 0.0069 \end{pmatrix}$$

This matrix helps in adjusting the estimated state based on the differences between actual and estimated outputs, enhancing the accuracy of state estimation.

D. Complete Output-feedback Controller

Combining the controller and estimator, the closed loop dynamics can be defined as

$$\dot{\tilde{x}} = \tilde{A}\tilde{x} + \tilde{B}r$$
$$\tilde{y} = \tilde{C}\tilde{x}$$

where $\dot{\tilde{x}} = [W, S, T, W_{error}, S_{error}, T_{error}]^T$ for this system. Analysis of the system yields the following matrices:

$$\tilde{A} = \begin{bmatrix} A - BK & BK \\ 0 & A - LC \end{bmatrix}$$
$$\tilde{B} = \begin{bmatrix} BK_r \\ 0 \end{bmatrix}$$
$$\tilde{C} = \begin{bmatrix} C & 0 \end{bmatrix}$$

which combined with the dynamics equations creates

$$\frac{d}{dt}\begin{bmatrix} x \\ e \end{bmatrix} = \begin{bmatrix} A - BK & BK \\ 0 & A - LC \end{bmatrix}\begin{bmatrix} x \\ e \end{bmatrix} + \begin{bmatrix} BK_r \\ 0 \end{bmatrix} r$$

E. Simulate Output-feedback Controller

This section explores combining various Luenberger estimators and errors to analyze how the system behaves under various conditions. To simulate the behavior of the system and estimate its states, we generated multi-channel input signals (`u1`, `u2`, `u3`) for the system and added Gaussian noise to the output signal (`y`). Using the modified system shown in the previous section for state estimation by adjusting the system matrices using the observer gain matrix (L) using different desired eigenvalues p. We simulated the state estimation using the modified system with the noisy output signal and input signals. A good estimator will show as close as possible behaviour to the actual output.

This process facilitates the understanding of the system's behavior and the estimation of its states using the observer-based approach.

F. State Estimation using Luenberger Observer

In the following case studies, the Luenberger estimator's performance is observed by altering the eigenvalues (p_1, p_2, and p_3) while maintaining the same error values.

Case 1 - Luenberger Estimator with p_1: For the initial case study, the eigenvalues (p_1) were set as:

$$p_1 = \begin{pmatrix} -5 \\ -4 + 5i \\ -4 - 5i \end{pmatrix}$$

Figure 14 demonstrates the system's behavior using p_1 for estimation.

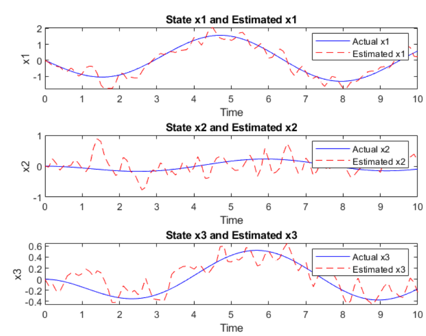

Fig. 14: System behavior with p_1

Case 2 - Luenberger Estimator with p_2: In the second scenario, the Luenberger estimator was adjusted with different eigenvalues (p_2):

$$p_2 = \begin{pmatrix} -5 \\ -4 + 0.05i \\ -4 - 0.05i \end{pmatrix}$$

Figure 15 illustrates the system's behavior using p_2 for estimation.

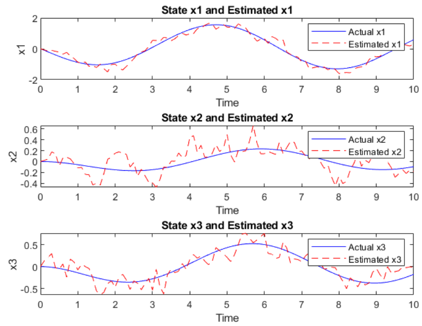

Fig. 15: System behavior with p_2

Case 3 - Luenberger Estimator with p_3: Finally, exploring another scenario, the Luenberger estimator was configured with yet another set of eigenvalues (p_3):

$$p_3 = \begin{pmatrix} -1 \\ -4 + 0.05i \\ -4 - 0.05i \end{pmatrix}$$

Figure 16 showcases the system's behavior using p_3 for estimation.

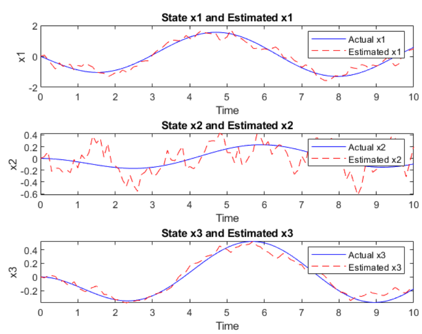

Fig. 16: System behavior with p_3

Observation and Analysis

By altering the eigenvalues (p) while maintaining consistent error values, we observed changes in the Luenberger estimator's performance. The estimations generated from these variations were compared with the actual system behavior. The investigation aims to determine the impact of different eigenvalues on the accuracy of state estimation.

We found that p_3 was the best performing however we also noted that x_2 the Salmon is sensitive to noise. Hence our observer matrix is:

$$L = \begin{pmatrix} 4.18 & 0.19 & 0.36 \\ -0.55 & 3.57 & 0 \\ -0.700 & 0 & 0.30 \end{pmatrix}$$

VII. System Control Design in the Frequency Domain

This section will explore the system's performance in the frequency domain and design an optimal system controller. By leveraging frequency domain techniques, the team can tailor a control system to meet specific performance requirements, ensuring stability, robustness, and optimal steady state behavior.

Topics covered will include transfer functions, frequency response analysis, Bode plots, Nyquist diagrams, and the Nyquist stability criterion. Additionally, the section will explore how these tools facilitate the design of controllers, enabling the team to achieve desired system performance across a range of frequencies.

A. Block Diagram

First, the system will be simplified to model a single-input single-output system (SISO). This system will include three external signals - reference signal, disturbance, and measurement noise. Both the single-input and single-output are chosen to be the population of whitefish. The disturbance signal represents a removal of whitefish from the population.

The following state-space representation of this new SISO model comes from the closed-loop controller in Section V-C. The A matrix represents the state matrix. B is a single column vector representing the input to the system, which is the population of whitefish. C represents the system output in terms of the state space variables. D is the direct transmission matrix, which is set to zero here.

$$A = \begin{bmatrix} -3 & -1.5 & 0 \\ 1.5 & -3.0 & 0 \\ 0 & 0 & -2.0 \end{bmatrix}$$
$$B = \begin{bmatrix} 0.2667 \\ 0.133 \\ 0 \end{bmatrix}$$
$$C = \begin{bmatrix} 1 & 0 & 0 & 0 \end{bmatrix}$$
$$D = 0$$

The block diagram for this simplified system is shown in figure 17.

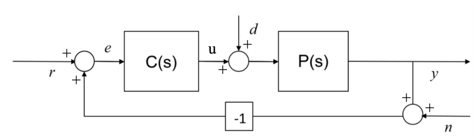

Fig. 17: Block diagram of the single-input single-output system

The Plant transfer function $P(s)$ is calculated using

$$P(s) = C(sI - A)^{-1}B$$

and it represents the transfer function from u to y. This gives:

$$P(s) = \frac{0.2667s^3 + 2.2s^2 + 6.601s + 6.752}{s^4 + 12s^3 + 58.5s^2 + 135s + 126.6}$$

This transfer function has four poles and three zeros:

- Poles: $-3.0 + 1.5i, -3.0 - 1.5i, -3.0 + 1.5i, -3.0 - 1.5i$
- Zeros: $-3.0 + 1.5i, -3.0 - 1.5i, -2.2503$

All of the above values are negative, so there are no zeros or poles in the right hand plane (RHP). This indicates that the system is stable under the current conditions. To further analyze the system, the Bode plot for $P(s)$ is shown in figure 18. The Bode plot shows infinite gain and phase margins and overall good stability of the system.

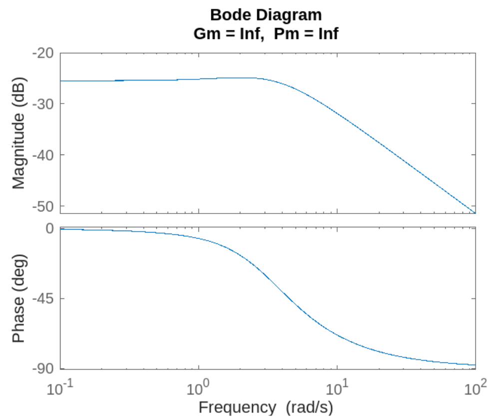

Fig. 18: Bode Plot of Plant transfer function

B. Studying Performance of PID Control

The next step in the control design process is to design an actual controller for the system. A very common control design technique is PID control which includes proportional, integral, and derivative control parameters. In fact, more than 95% of industrial control problems implement a PID controller to solve them due to its capability to solve a wide range of control problems [14].

A variety of PID control parameters were tested to observe their effects on the system, and the results are presented in the following graphs.

Controller 1: The first controller is tuned using the following parameters:

$$k_p = 10$$
$$k_i = 10$$
$$k_d = 10$$

These parameters resulted in a controller of the form:

$$C(s) = 10 + \frac{10}{s} + 10s$$

for which the Bode plot and step response are shown in figures 19 and 20.

As seen in the bode plot, the gain margin is infinite and the phase margin is 120 degrees, indicating robust control.

The step response indicates fairly good tracking behavior. There is no overshoot, the settling time is 9.2442 seconds, and the steady state error is 0.00053%.

Controller 2: The second controller is tuned using the following parameters:

$$k_p = 1$$
$$k_i = 1$$
$$k_d = 1$$

These parameters resulted in a controller of the form:

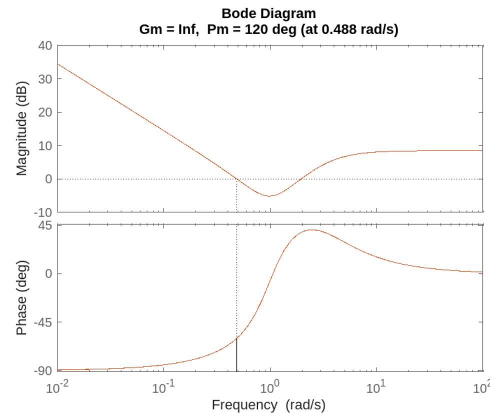

Fig. 19: Bode Plot for Controller 1

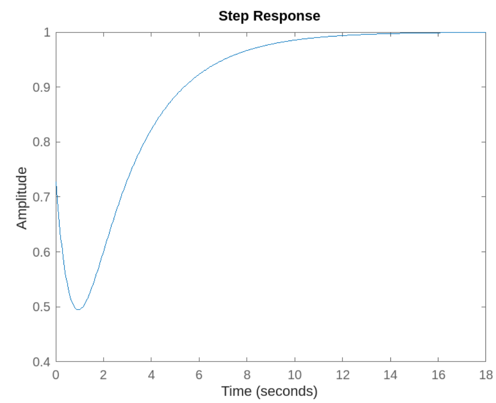

Fig. 20: Step Response for Controller 1

$$C(s) = 1 + \frac{1}{s} + 1s$$

for which the Bode plot and step response are shown in figures 21 and 22.

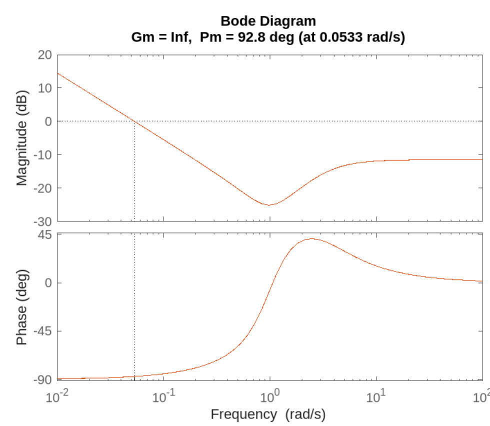

Fig. 21: Bode Plot for Controller 2

The Bode plot shows infinite gain margin and a phase margin over 90 degrees, indicating less robustness than *Controller 1*.

The step response indicates good tracking behavior. There is no overshoot, the settling time is 75.8804 seconds, and the steady state error is 0.0032%. Overall, this controller has worse performance when compared to *Controller 1*.

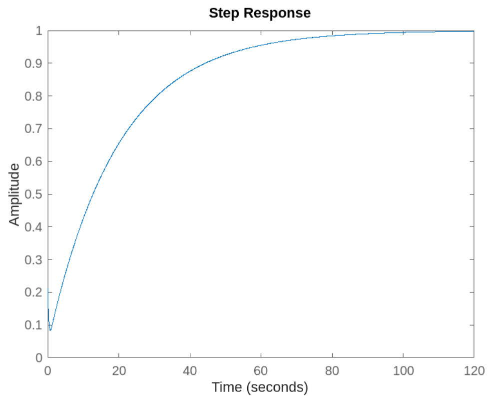

Fig. 22: Step Response for Controller 2

Knowing how higher PID parameter values affects the system, it's time to design controllers with varying amounts of each parameter to find the optimal solution.

Controller 3-5: The next three controllers are tuned using the following parameters:

	k_p	k_i	k_d
Controller 3	10	1	15
Controller 4	15	10	1
Controller 5	1	15	10

TABLE III: PID Parameters used for Controllers 3-5

These parameters resulted in a controller of the form:

$$C(s) = k_p + \frac{k_i}{s} + k_d s$$

for which the Bode plot and step response are shown in figures 23 and 24.

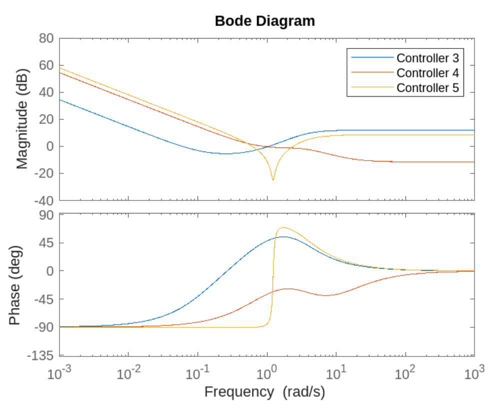

Fig. 23: Bode Plot for Controllers 3-5

All three controllers showed infinite gain margins and phase margins greater than 90 degrees, which indicates robust control.

The response behavior of each controller is described in the following table:

Controller 5 demonstrated the shortest settling time and smallest steady state error. However, it was the only controller of the three to have nonzero overshoot. Since the controllers showed relatively similar behavior, it was decided to look at each parameter individually to determine if only one parameter was necessary for robust control.

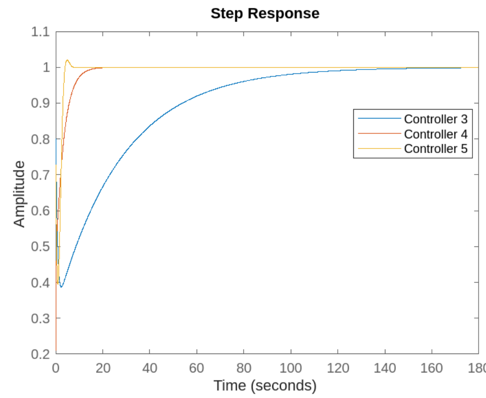

Fig. 24: Step Response for Controllers 3-5

	Tracking Behavior	**Overshoot**	**Settling Time**	**Steady State Error**
Controller 3	Good	0	99.20 s	0.0018%
Controller 4	Good	0	11.04	0.0020%
Controller 5	Good	1.995	3.6776	0.0007%

TABLE IV: PID Parameters used for Controllers 3-5

Controller 6-8: The next three controllers are tuned using the following parameters:

	k_p	k_i	k_d
Controller 6	10	0	0
Controller 7	0	10	0
Controller 8	0	0	10

TABLE V: PID Parameters used for Controllers 6-8

These parameters resulted in a controller of the form:

$$C(s) = k_p + \frac{k_i}{s} + k_d s$$

for which the Bode plot and step response are shown in figures 25 and 26.

All three controllers showed infinite gain margins. Controller 6 demonstrated infinite gain margin, controller 7 had a phase margin of 87 degrees, and controller 8 had a phase margin of -104 degrees.

Controller 7 (integral control) demonstrated the most robust behavior with no overshoot, a steady state error of 0.0032%, and a settling time of 7.1252 seconds.

C. *Designing a Feedback Control that Follows Specifications*

The success of a controller is determined by predetermined benchmarks. Here, three benchmarks were determined as follows:

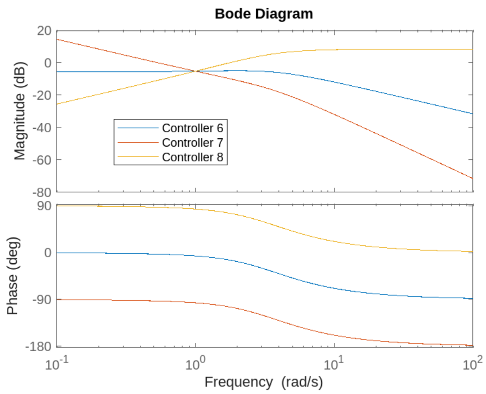

Fig. 25: Bode Plot for Controllers 3-5

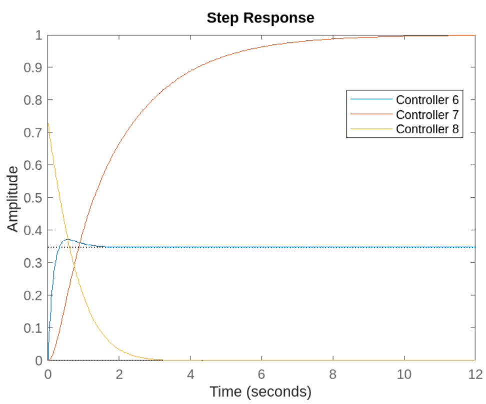

Fig. 26: Step Response for Controllers 3-5

- Steady-state error less than 1%, such that $|\frac{1}{1+L(s)}| < 0.01$ at $s = 0$ where $L(s) = P(s)C(s)$ and $C(s)$ is the controller
- Tracking error less than 25% from 0 to 1 rad/s, such that $|\frac{1}{1+L(s)}| < 0.25$ during this range of frequencies
- Phase margin of at least 30°

Using MATLAB's Control System Designer, the following PI controller was designed to fit the required parameters:

$$C(s) = \frac{44.309(s+3.864)}{s}$$

The system already had a mostly favorable step response, but the steady-state value was below 1. The proportional controller was added to satisfy the tracking error requirement and the integral controller was added to decrease the steady-state error in the system.

Figure 27 plots the step response of the SISO system under this controller.

The bode plot indicates that the required specifications have been met. The 2% steady state error corresponds to minimum 34 dB initial magnitude, which is below the true initial value. The 10% tracking error corresponds to 20 dB, meaning that the magnitude of the plot must remain above 20 dB for times between 0 and 1 second. This is certainly met. Lastly, the phase margin is 90 deg and the gain margin is infinite, which infers robust control.

Next, the closed loop control is analyzed. Closed loop control follows the transfer function below.

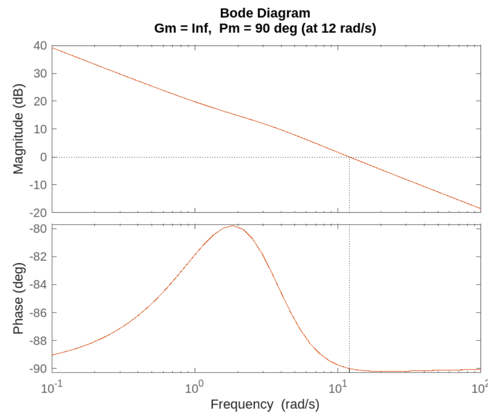

Fig. 27: Bode Plot for PI Controller

$$G_{r-y} = \frac{L}{1+L} \text{ where } L = PC$$

The following bode and step responses (figures 28 and 29) are developed for this closed loop transfer function.

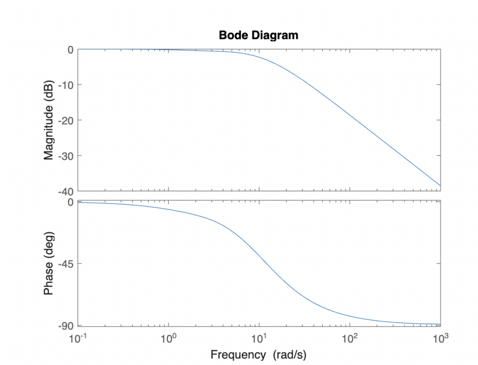

Fig. 28: Bode Plot for Closed-Loop PI Controller

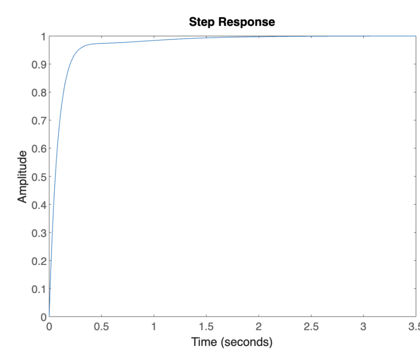

Fig. 29: Step Response for Closed-Loop PI Controller

The bode diagram demonstrates infinite gain margin for the closed-loop transfer function. The closed-loop step response is very smooth, with an overshoot of 0, a steady state error of 0.0002%, a rise time of 0.1914 seconds, and a 0.8394 second settling time. This controller is very responsive and robust.

D. Closed-Loop Disturbance Analysis

Now that a controller has been designed to satisfy the given specifications, we can then analyze how it behaves when a disturbance is introduced to the system.

The closed-loop transfer function between the disturbance and output was calculated using the following equation

$$G_{dy} = \frac{P}{1+L}$$

The fully calculated transfer function is shown below in figure 30.

```
G_dy =

          0.2667 s^8 + 5.401 s^7 + 48.61 s^6 + 250.7 s^5 + 798 s^4 + 1565 s^3 + 1747 s^2 + 854.5 s
  ---------------------------------------------------------------------------------------------------
  s^9 + 35.82 s^8 + 546 s^7 + 4752 s^6 + 2.635e04 s^5 + 9.711e04 s^4 + 2.39e05 s^3 + 3.795e05 s^2 + 3.53e05 s
                                                                                              + 1.463e05
```

Fig. 30: G_{dy} Transfer Function

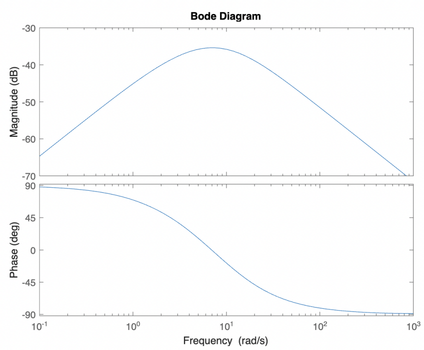

Fig. 31: Bode Plot of G_{dy} Transfer Function

As seen in the response of the system to low frequency, the system is most sensitive to disturbances in the range of $10^{-1}\frac{rad}{s}$ to $10\frac{rad}{s}$. Given that we want G_{dy} to be small at large frequencies, our current model satisfies this and shows a good response to disturbance.

For such a control system, an ecosystem should be robust to disturbances including weather, human-induced pressure, and other natural factors. An ideal controlled system such as this would be able to encounter external disturbances without becoming unstable.

The effect of a disturbance on the system was further analyzed by simulating three different values of frequency (ω) for a disturbance of the form $d(t) = sin(\omega t)$. The MATLAB function *tf2ss* was used to get the [A,B,C,D] matrix for the transfer function G_{dy}, and then *lsim* was used to simulate the disturbance response.

$\omega = 0.5rad/s$

The system's response is very minimally impacted by external response as shown in figure 32. A low frequency input disturbance signal translates to a low frequency, low amplitude response.

$\omega = 5rad/s$

The system's response is very minimally impacted by external response as shown in figure 33. A low frequency input disturbance signal translates to a low frequency, low amplitude response. Compared to the previous simulation ($\omega = 0.5rad/s$), the system response demonstrates more oscillatory behavior that is in phase with the disturbance signal.

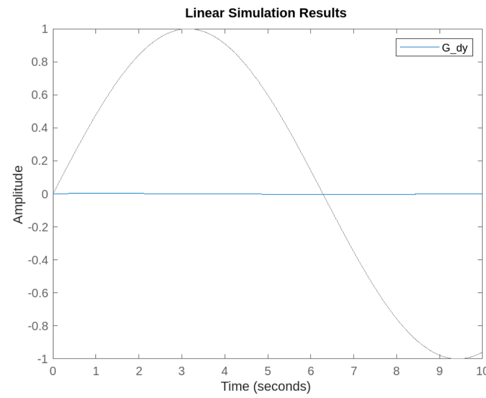

Fig. 32: Linear Simulation of a Sinusoidal Disturbance Signal with $\omega = 0.5$

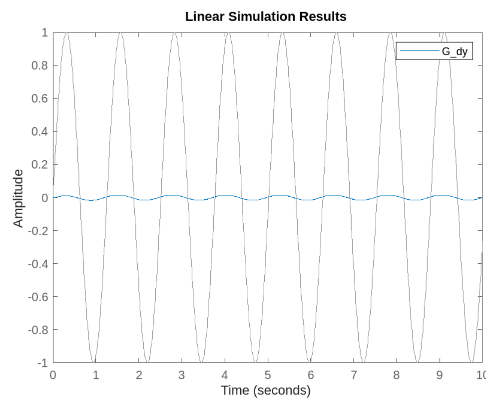

Fig. 33: Linear Simulation of a Sinusoidal Disturbance Signal with $\omega = 5$

$\omega = 50rad/s$

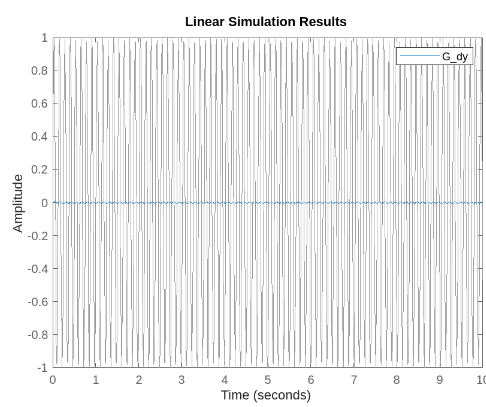

Fig. 34: Linear Simulation of a Sinusoidal Disturbance Signal with $\omega = 50$

As shown in the previous three plots, our controller is very robust and not sensitive to sinusoidal external disturbance.

E. Closed-Loop Noise Analysis

The system's response to noise was then analyzed using a Gaussian noise input signal. The closed-loop transfer function from the noise signal to the output signal was calculated using the following equation.

$$G_{ny} = \frac{-L}{1+L}$$

Using the open-loop transfer function $L(s)$, G_{ny} is computed to be:

```
G_ny =

    -11.82 s^9 - 285 s^8 - 3078 s^7 - 1.943e04 s^6 - 7.828e04 s^5 - 2.06e05 s^4 - 3.453e05 s^3 - 3.37e05 s^2 - 1.463e05 s
  ------------------------------------------------------------------------------------------------------------------------
  s^10 + 35.82 s^9 + 546 s^8 + 4752 s^7 + 2.635e04 s^6 + 9.711e04 s^5 + 2.39e05 s^4 + 3.795e05 s^3 + 3.53e05 s^2 + 1.463e05 s
```

Fig. 35: Transfer function G_{ny}

To simulate the system's sensitivity to noise, two plots were created. The first was the Bode plot for the transfer function G_{ny} shown in figure 36. The second plot was a linear simulation using MATLAB's *lsim* function with a Gaussian noise signal. The Gaussian signal was created by generating a random set of values between 0 and 1 for a duration of 1000 seconds. The system was then plotted in figure 37 over this time range and compared to the input noise signal for five trials.

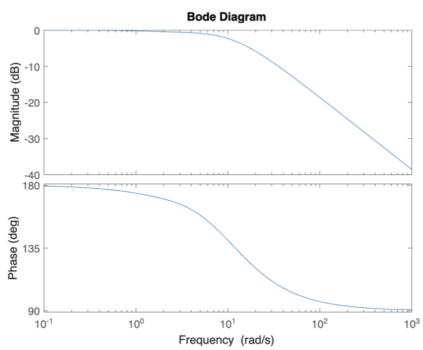

Fig. 36: Bode plot for G_{ny}

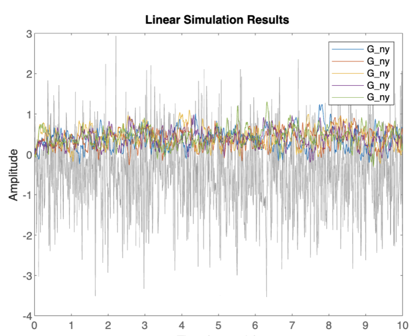

Fig. 37: Linear Simulation of a Gaussian Noise Signal

The system responds well to a noise signal since the amplitude of the responses is very minimal compared to the amplitude of the noise signal. However, the system has a more robust response to disturbance signals when compared to noise signals.

VIII. Discussion and Conclusion

Our three species predator-prey-invasive species model, revealed a stable ecosystem with 3,075,198 whitefish, 1,033267 salmon, and 1,644,874 lake trout without control input. Various PID control conditions were implemented to help develop harvest quotas for biologists responsible for maintaining desired ecosystem dynamics. A PI controller was sufficient to satisfy the specifications minimizing steady state and tracking errors and maximizing phase margin while being robust to noise and disturbance. Ecosystems must be able to absorb disturbances without collapsing. The objective of our study was to help develop quotas or standards for fish harvesting in a simplified ecosystem model.

The controller developed herein can be used as a framework on which to develop fish harvesting regulations. To that end, our results must be translated to metrics that fish and wildlife management agencies can implement. Future developments would do just that–depending on the specific goals of each agency. The process for doing this adheres to the following basic outline. First, the harvest quotas and desired species populations must be established. Then, a mapping function must be established to translate the PID output to those desired harvest parameters. Here, our controller is already in the desired units: harvest, so only the magnitude must be manipulated.

Lastly, given the continuous-signal implementation of the PID controllers developed in this report and the uncertainty in species population metrics, our controller is not an ideal representation of true, actionable management practices. Measuring species populations is a cumbersome, time-consuming process involving multiple simplifications. It is unreasonable to assume that accurate, real-time measurements on population sizes and distributions can be made for large ecosystems. In reality, fish populations are measured through mark and recapture studies, electrofishing and fish netting, and field surveys, which periodically inform updates on fish populations. This explains why our PID response is much quicker than expected in reality. It follows a time scale of seconds, where days or even months are more realistic. Future control models will comply with the population measurement capabilities of the agencies implementing them, as well as their budget and other such factors.

IX. Acknowledgements

We would like to thank Professor Na Li and the rest of the teaching staff: Yuyang Zhang, Haitong Ma, Arjun Batra, and Melinda Modisette for their feedback and advice throughout the semester on this project.

Appendix A
Nonlinear System Dynamics Exploration

For the entirety of our closed-loop system dynamics exploration previously discussed in this report we used our LTI system as our model. However, our original system was nonlinear and does not have the same behavior as our linearized model. To explore the nonlinear system dynamics, we used the feedback controller designed in Section V-C. As a reminder, the feedback controller was designed with the gain matrix (K):

$$\begin{bmatrix} -3.1768 & -1 & 0.7 \\ 1.3655 & -2.59 & 0 \\ -0.3691 & 0 & -1.31 \end{bmatrix}$$

Using *ode45* in MATLAB, a time domain simulation was conducted and the results are plotted in figure 38.

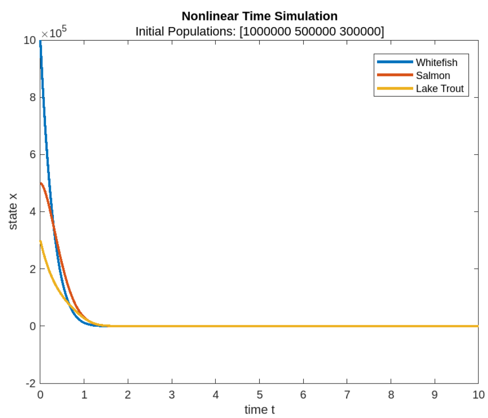

Fig. 38: Nonlinear Time Domain Simulation

This controller indeed stabilizes the system. However, the stabilization is not ideal since all of the fish populations go to zero.

References

[1] A. Supartini, T. Oishi, and N. Yagi, "Changes in fish consumption desire and its factors: A comparison between the United Kingdom and Singapore," Foods (Basel, Switzerland), https://www.ncbi.nlm.nih.gov/pmc/articles/PMC6068685/ (accessed Oct. 8, 2023).

[2] Daniel O'Keefe, "How much do Lake Trout and chinook salmon really eat?," MSU Extension, https://www.canr.msu.edu/news (accessed Oct. 8, 2023).

[3] "Fisheries management and Ecology - Wiley Online Library," Catchability of Atlantic salmon at high water temperatures: Implications for river closure temperature thresholds to catch and release angling, https://onlinelibrary.wiley.com/doi/abs/10.1111/fme.12651 (accessed Oct. 8, 2023).

[4] G. Gunkel and ht. Kausch, "Feeding and growth of Fry and fingerlings of Whitefish, Coregonus fera J.," EIFAC Workshop on Mass Rearing of Fry and Fingerlings of Freshwater Fishes. Papers (1979), https://www.fao.org/3/ae993e/AE993E18.htm (accessed Oct. 8, 2023).

[5] H. R. and M. Roser, "Fish and overfishing," Our World in Data, https://ourworldindata.org/fish-and-overfishing (accessed Oct. 8, 2023).

[6] J. Lenart and D. C. Carrofino, Technical Fisheries Committee Administrative Report 2018: Status of Lake Trout and Lake Whitefish Populations in the 1836 Treaty-Ceded Waters of Lakes Superior, Huron, and Michigan, with Recommended Yield and Effort Levels for 2018, https://www.michigan.gov/-/media/Project/Websites/dnr/Documents/Fisheries/Status/folder2/2014 StatusStocksReport.pdf?rev=566fe2c9cb0e434f8186019aecdff884 (accessed Oct. 8, 2023).

[7] Kumar, S., Kumar, A., Abdel-Aty, A.-H., amp; Alharthi, M. L. (2021, March 27). A study on four-species fractional population competition dynamical model. Results in Physics. https://www.sciencedirect.com/science/article/pii/S2211379721002473

[8] K. Walker and A. Barilotti, "Ocean Whitefish Enhanced Status Report," CA Marine Species Portal, https://marinespecies.wildlife.ca.gov/ocean-whitefish/the-species/ (accessed Oct. 8, 2023).

[9] "Lake Whitefish," Lake Whitefish: Species Information: Fisheries: Fish & Wildlife: Maine Dept of Inland Fisheries and Wildlife, https://www.maine.gov/ifw/fish-wildlife/fisheries/species-information/lake-whitefish.html (accessed Oct. 8, 2023).

[10] L. Brannian, "Alaska Department of Fish and Game," The Estimation of Daily Escapement and Total Abundance from Catch per Unit Effort of the Sockeye Salmon Fishery in Togiak Bay, Alaska, https://www.adfg.alaska.gov/FedAidpdfs/afrbIL.226.pdf (accessed Oct. 8, 2023).

[11] Rutherford, Evaluation of natural reproduction, stocking rates, and fishing regulations for steelhead Oncorhynchus mykiss, chinook salmon O. tschawytscha, and coho salmon in Lake Michigan, https://www.dnr.state.mi.us/PUBLICATIONS/PDFS/ifr/ifrhome /federalaid/inland/F-35-R-22/650-97.pdf (accessed Oct. 8, 2023).

[12] U.S. Fish & Wildlife Service Mass Marking Program - Wisconsin DNR. Mass Marketing Program Lake Trout . (2021). https://dnr.wisconsin.gov/sites/default/files/topic/Fishing/L_GreatLakes MassMarking2022ChinookSalmonWildProduction.pdf

[13] Zink, T. Brenden, S. Valle de Suza, T. Cwalinski, and R. Claramunt, "Status of a stocked Atlantic salmon population in Lake Huron," Journal of Great Lakes Research, https://www.sciencedirect.com/science/article/abs/pii/S0380133023000 850 (accessed Oct. 8, 2023).

[14] Astrom, K. J., amp; Murray, R. M. (2021). Feedback systems: An introduction for scientists and Engineers (Second, Vol. 3.1.5). Princeton University Press.